

SPIN EXCITATIONS IN LOCALIZED AND ITINERANT MAGNETS

B. ROESSLI

Laboratory for Neutron Scattering
Paul Scherrer Institut and ETH Zurich
CH-5232 Villigen, PSI, Switzerland

P. BÖNI

Physik-Department E21, Technische Universität München
D-85748 Garching, Germany

October 30, 2018

Abstract

Collective excitations in magnetic materials can be investigated by means of inelastic neutron scattering. We show that this experimental method gives access to the complete spectrum of magnetic fluctuations through the energy- and momentum-dependence of the dynamical susceptibility. We focus on the dynamical properties of magnets with localized spin densities and of metals. From such studies, microscopic parameters like exchange integrals, spin-wave stiffness and relaxation times can be determined. This is of great help to test current theories in magnetism.

1 Introduction

Many materials exhibit a spontaneous phase transition from a paramagnetic state to an ordered configuration of their magnetic moments below some critical temperature. This cooperative phenomenon is found in a wide range of materials, like insulators, metals, superconductors, heavy fermion systems, and so on. Ordered magnetic states can be classified as weak or strong ferromagnets, antiferromagnets, ferrimagnets, and incommensurate structures. Magnetic ordering originates from electrostatic interactions which induce correlations between the electrons. An exact mathematical treatment of the Coulomb interaction involving many electrons together with the Pauli-principle has been, up to now, an impossible task. Accordingly, some simplifications of the problem have to be made. An effective many-body Hamiltonian which takes into account both the kinetic energy of the electrons and the Coulomb interaction has been derived by Hubbard [1]. Considering a single-electron band and neglecting inter-atomic interactions, the Hubbard model is given by

$$H = -t \sum_{i,j} \sum_{\sigma} (c_{i\sigma}^{\dagger} c_{j\sigma} + c_{i\sigma} c_{j\sigma}^{\dagger}) + U \sum_j n_{j\uparrow} n_{j\downarrow}. \quad (1)$$

The first term describes electrons hopping through the lattice, while the interaction term describes the Coulomb repulsion between electrons in the same orbital,

$$U = \int d\vec{r}_1 \int d\vec{r}_2 |\phi(\vec{r}_1)|^2 \frac{e^2}{|\vec{r}_1 - \vec{r}_2|} |\phi(\vec{r}_2)|^2. \quad (2)$$

$|\phi(\vec{r}_{1,2})|^2$ are the charge densities.

If the kinetic energy dominates ($t \gg U$), the Hubbard model describes ferromagnetism in metallic systems. On the other hand, in the limit of large Coulomb interactions ($U \gg t$) and at half-filling Eq. 1 reduces to

$$H = J \sum_{i,j} \vec{S}_i \cdot \vec{S}_j, \quad (3)$$

with J equal to $J = 4t^2/U$ (see Ref. [2]). Equation 3 is the Heisenberg model. It shows that the magnetic interactions in solids can be described by the mutual interaction of pairs of spins \vec{S} which are coupled together by the exchange integral J . Derived from the Hubbard

model, Eq. 3 favors an antiferromagnetic ground state as the energy is minimized for anti-parallel spins. However it has the same form as the Hamilton operator originally derived by Heisenberg for ferromagnets. The Heisenberg model is therefore expected to be valid for positive and negative values of the exchange integral J .

Neutron scattering is the only method that allows to determine both the spatial and time correlations of the magnetic excitations through the dipolar coupling of the magnetic moment of the neutron with the unpaired electrons of the sample,

$$\frac{d^2\sigma}{d\Omega dE} = \frac{k_f}{k_i} (\gamma r_0 \frac{1}{2} g F(\vec{Q}))^2 \sum_{\alpha\beta} (\delta_{\alpha\beta} - \hat{Q}_\alpha \hat{Q}_\beta) S^{\alpha\beta}(\vec{Q}, \omega). \quad (4)$$

$\gamma = -1.913$ is the gyromagnetic ratio, $r_0 = 0.2818 \cdot 10^{-12}$ cm is the classical radius of the electron, g the Landé splitting factor, k_i and k_f are the wavenumbers of the incident and scattered neutrons, and $F(\vec{Q})$ is the form factor. \hat{Q} is the scattering vector normalized to unity and $S^{\alpha\beta}(\vec{Q}, \omega)$ the magnetic scattering function. $S^{\alpha\beta}(\vec{Q}, \omega)$ is related to the imaginary part of the wavevector and frequency dependent susceptibility through the fluctuation-dissipation theorem by

$$S^{\alpha\beta}(\vec{Q}, \omega) = \frac{\hbar}{\pi} \frac{1}{(1 - \exp(-\hbar\omega/k_B T))} \Im \chi(\vec{Q}, \omega). \quad (5)$$

This implies that the magnetic moment of the neutron acts as a wavevector and frequency dependent magnetic field that probes the dynamic magnetic response of the sample.

2 Collective spin excitations in localized magnets

2.1 Spin Waves in the Ferromagnetic Heisenberg Model

At zero temperature, every spin in a ferromagnet points along the same direction, i.e. along the magnetization \vec{M} . The ground-state can therefore be written as $|\uparrow\uparrow\uparrow \dots\rangle$. The saturation magnetization of the sample is accordingly given by $M_0 = Ng\mu_B S$. Upon increasing the temperature, the magnetization decreases indicating deviations of

the spins from their parallel alignment, i.e. $S_j^z \rightarrow S_j^z - 1$. In the quantum-mechanical formalism, this is achieved by the annihilation operator S_j^- that reduces the spin component S^z at the spin position j . If $S = 1/2$, this yields $S_j^- | \uparrow \uparrow \uparrow \dots \rangle = | \uparrow \uparrow \uparrow \dots \downarrow \uparrow \dots \rangle$. As the spins are coupled by the exchange interaction, the excitation will propagate through the crystal like a wave. Because the crystal lattice is periodic in space, it is of advantage to introduce the Fourier transform of the exchange interaction and spin operator, namely $J(\vec{r}_{i,j}) = J(\vec{r}_i - \vec{r}_j) = \frac{1}{N} \sum_{\vec{k}} J(\vec{k}) \exp(i\vec{k} \cdot \vec{r}_{i,j})$, $S_j^z = \sum_{\vec{k}} S_{\vec{k}}^z \exp(-i\vec{k} \cdot \vec{r}_{i,j})$, and $S_j^{+,-} = S_j^x \pm S_j^y = \sum_{\vec{k}} S_{\vec{k}}^{+,-} \exp(\mp i\vec{k} \cdot \vec{r}_j)$. Accordingly, the Heisenberg operator transforms into

$$H = N \sum_{\vec{k}} J(\vec{k}) [S_{\vec{k}}^z S_{-\vec{k}}^z + \frac{1}{2} (S_{\vec{k}}^+ S_{-\vec{k}}^- + S_{\vec{k}}^- S_{-\vec{k}}^+)]. \quad (6)$$

Using the commutation relations between the spins $[S_k^+, S_q^-] = 2S_k^z \delta_{k,q}$ and $[S_k^{+,-}, S_q^z] = \mp 2S_k^{+,-} \delta_{k,q}$, the dispersion relation of the magnetic excitations is given by the solution of the equation of motion $i\hbar \frac{\partial}{\partial t} S_k^-(t) = [S_k^-, H]$. This is achieved within the 'linear' approximation by setting $[S_k^+, S_q^-] \simeq \delta_{k,q} 2S$, i.e. it is assumed that the spin deviations from their maximal value are small. This approach is valid at low temperatures $T \rightarrow 0$. As we will see below, the 'linear' approximation breaks down when the magnetic fluctuations are large, and in particular when the temperature is close to the Curie temperature T_c . Making use of the '*Ansatz*' $S_{\vec{k}}^-(t) = e^{i\omega(\vec{k})t} S_{\vec{k}}^-$, the dispersion relation for the spin waves in an isotropic ferromagnet is obtained

$$\hbar\omega(\vec{k}) = 2S(J(0) - J(\vec{k})). \quad (7)$$

Equation 7 shows that the dispersion of the magnetic excitations is a function of the Fourier transform of the exchange integrals between the spins. For small values of \vec{k} , the dispersion is quadratic $\hbar\omega(\vec{k}) = Dk^2$ with a stiffness constant $D = 2SJa^2$ (a is the lattice constant). For a cubic crystal D has the same value for all directions of k .

2.1.1 Neutron-Scattering Cross-Section

The inelastic scattering of neutrons allows to measure the dispersion relation $\omega(\vec{k})$ given in Eq. 7 directly, as [3] the magnetic neutron cross

section is equal to (see Eq. 4)

$$\begin{aligned} \frac{d^2\sigma}{d\Omega dE} &= 0.2916 \cdot 10^{-24} \frac{k_f}{k_i} \left(\frac{1}{2} gF(\vec{Q})\right)^2 \exp(-2W(\vec{Q})) \\ &\times \left\{ (1 - Q_z^2) \frac{1}{2\pi\hbar} \int_{-\infty}^{\infty} dt \exp(-i\omega t) \langle S_{\vec{Q}}^z S_{-\vec{Q}}^z(t) \rangle \right. \\ &\left. + \frac{1}{4} (1 + Q_z^2) \frac{1}{2\pi\hbar} \int_{-\infty}^{\infty} dt \exp(-i\omega t) \langle S_{\vec{Q}}^+ S_{\vec{Q}}^-(t) + S_{-\vec{Q}}^+ S_{-\vec{Q}}^-(t) \rangle \right\}. \end{aligned} \quad (8)$$

Here, $W(\vec{Q})$ is the Debye-Waller factor. The scattering vector \vec{Q} is related to the spin-wave wave-vector \vec{k} through the relation $\vec{Q} = \vec{\tau} + \vec{k}$, where $\vec{\tau}$ is a reciprocal lattice vector. The neutron-scattering cross-section for the isotropic ferromagnet is obtained by evaluating the thermal averages $\langle \dots \rangle$ in Eq. 8. Within the spin-wave approximation, $\langle S_{\vec{Q}}^z S_{-\vec{Q}}^z(t) \rangle$ does not depend on time and hence gives no contribution to the inelastic scattering, while $\langle S_{\vec{Q}}^+ S_{\vec{Q}}^-(t) \rangle = 2SN[\exp(\frac{\hbar\omega}{k_B T}) - 1]^{-1} = 2SNn_{\vec{k}}$ [3]. Accordingly, Eq. 8 reduces to

$$\begin{aligned} \frac{d^2\sigma}{d\Omega dE} &= 0.2916 \cdot 10^{-24} \frac{k_f}{k_i} \left(\frac{1}{2} gF(\vec{Q})\right)^2 \exp(-2W(\vec{Q})) \\ &\times \frac{1}{2} S \frac{(2\pi)^3}{v_0} \sum_{\vec{k}, \vec{\tau}, \pm} \left(n_{\vec{k}} + \frac{1}{2} \pm \frac{1}{2}\right) \delta(\hbar\omega_{\vec{k}} \mp \hbar\omega) \delta(\vec{Q} \mp \vec{k} - \vec{\tau}) \end{aligned} \quad (9)$$

2.1.2 Example

The insulators EuS and EuO are typical examples of ferromagnets which are well described by the isotropic Heisenberg Hamiltonian. The electronic configuration of the 4f electrons of Eu^{2+} has a $^8S_{7/2}$ ground state and hence the magnetic moment is only due to the spin. These two insulators undergo a phase transition to an ordered ferromagnetic ground-state at $T_c=16.6\text{K}$ and $T_c=69\text{K}$, respectively. Results of spin-wave measurements and the corresponding spin-wave dispersion in EuS using the triple-axis method are shown in Fig.1 (taken from Refs. [4, 5]).

The Fourier transform of the exchange interactions

$$J(\vec{q}) = \sum_{i,j} J_{i,j} \exp(i\vec{q} \cdot \vec{r}_{i,j}) \quad (10)$$

can be easily calculated for a fcc lattice. The results of the calculations using Eq. 7 are given by the solid line in Fig. 1. As expected,

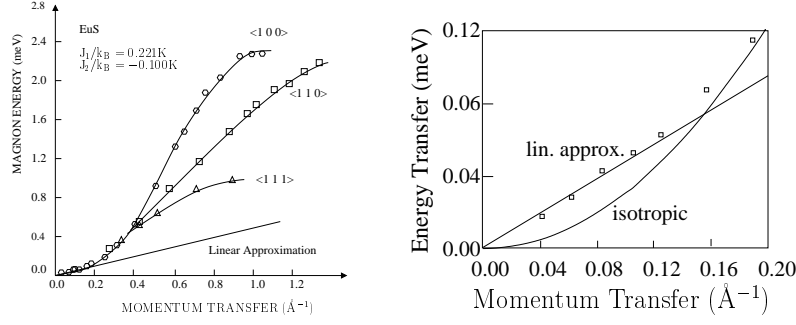


Figure 1: *Left*: Dispersion of the spin waves in EuS. *Right*: Expanded scale of the magnon dispersion in EuS, demonstrating the linear dispersion at small k values (after Refs. [4, 5]).

nearest-neighbor exchange interactions are strongest in EuS. However, magnetic interactions of a spin at an Eu^{2+} position with more distant spins is significant. Also, we point out that the sign of the magnetic interaction changes as a function of distance which suggests competing ferro- and antiferromagnetic exchange interactions in EuS.

The value of the Eu^{2+} magnetic moment at saturation is large, $\mu \sim 7\mu_B$, and dipolar interactions cannot be neglected. As dipolar interactions decay like $1/r^3$ and are anisotropic, they modify the spectrum of the spin-wave excitations [6]:

$$E(\vec{k}) = \{\hbar\omega(\vec{k})[\hbar\omega(\vec{k}) + g\mu_B\mu_0 M(T) \sin^2 \theta_{\vec{k}}]\}^{1/2}, \quad (11)$$

$\hbar\omega(\vec{k})$ denotes the dispersion relation of Eq. 7; μ_0 is the induction constant; $M(T)$ the magnetization and $\theta_{\vec{k}}$ the angle between the magnetization vector \vec{M} and \vec{k} . At small \vec{k} the dipolar interactions lead to a linear dispersion

$$E(\vec{k} \rightarrow 0) \simeq k\sqrt{Dg\mu_B\mu_0\vec{M}} \cdot \sin \theta_{\vec{k}}. \quad (12)$$

Fig. 1 shows results of a high-resolution experiment that demonstrates the linear dispersion in EuS due to dipolar interactions [5].

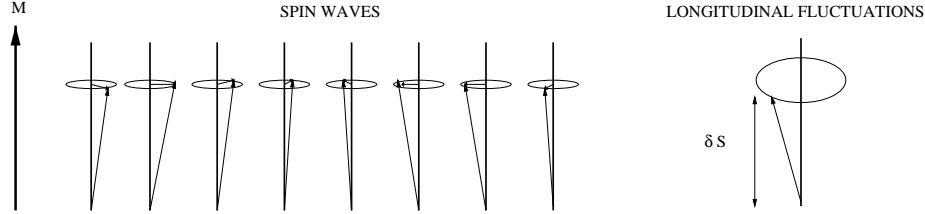


Figure 2: Schematic representation of a spin-wave excitation transverse to the magnetization \vec{M} (*left*) and of longitudinal fluctuations (*right*).

2.1.3 Longitudinal fluctuations

Spin-wave theory is based on the assumption that spin deviations from the equilibrium value are small and that the 'length' of the spin vector \vec{S} is a constant. This leads to the view that spin waves are unperturbed collective modes *transverse* to the magnetization \vec{M} . Close to the phase transition and in the paramagnetic phase, interactions between the spin-wave modes are important and fluctuations along the magnetization vector appear, as shown in Fig. 2. In the temperature regime below T_c where critical fluctuations are large, mode-mode coupling theory [7] predicts that the transverse spin components still disperse like $\omega(\vec{k}) = Dk^2$. The stiffness constant is given by $D = (4\pi\xi/a)^{-1/2}\sqrt{TJ}/\hbar a^2$ (ξ is the correlation length and a the lattice constant). In addition, the spin waves are damped in such a way that the δ -function in the neutron cross-section of Eq. 9 becomes a Lorentzian,

$$S(\vec{k}, \omega) = \omega(1 - \exp(-\omega/k_B T))^{-1} \chi_k^T \frac{\Gamma(\vec{k})}{(\omega \pm \omega(\vec{k}))^2 + \Gamma(\vec{k})^2} \quad (13)$$

where $\chi_k^T = 4\pi M^2 \xi N / (k^2 k_B T a^3)$ is the transverse susceptibility and $\Gamma = A k^{2.5} \xi^{3/2}$. For small wave-vectors k , the longitudinal part of the dynamical susceptibility is a diffuse central peak of Lorentzian-shape centered around zero-energy transfer and of width $\Gamma(\vec{k}) \sim k^{2.5}$,

$$S(\vec{k}, \omega) = \omega(1 - \exp(-\omega/k_B T))^{-1} \chi_k^L \frac{\Gamma(\vec{k})}{\omega^2 + \Gamma(\vec{k})^2}. \quad (14)$$

The static longitudinal susceptibility $\chi^L(\vec{k})$ behaves like $c_1 \frac{\xi/\gamma}{k} + (1 - c_1)(\xi/\gamma)^2$, where $\gamma \sim 1$ [7]. Measuring the longitudinal fluctuations with neutrons is however a difficult task, as when the temperature gets close to T_c , the spin-waves renormalise and merge with the central component. The best way to separate the longitudinal from the transverse components is to use polarization analysis, as explained in the next chapter.

2.1.4 Polarization analysis

In the following section, we shall give a brief description of how polarization analysis can be used to separate the transverse and longitudinal components of the dynamical susceptibility in ferromagnets. A more detailed discussion of the spin-dependent neutron cross-sections can be found in the book of Lovesey [3] and in the seminal paper of Blume [8]. The neutron cross-section for magnetic scattering contains terms that depend on the spin of the neutron. The term *polarization analysis* refers to the analysis of the spin-state of the neutron before and after the scattering process. This implies that for most practical cases (but not all!), the spin of the neutron before scattering has to be in a well defined state. The neutron cross-section for scattering by spin waves in a ferromagnet with a polarized beam is given by

$$\frac{d^2\sigma}{d\Omega dE} \propto [1 + (\hat{\vec{Q}} \cdot \hat{\vec{m}})^2 \pm 2(\vec{P}_0 \cdot \hat{\vec{Q}})(\hat{\vec{m}} \cdot \hat{\vec{Q}})] \quad (15)$$

where $\hat{\vec{m}}$ is a unit vector directed along the magnetization and \vec{P}_0 is the polarization vector of the neutrons before scattering by the sample. The \pm sign refers to spin-wave creation and annihilation, respectively. The final polarization of the neutron beam \vec{P} , i.e. after scattering, is [9]

$$\vec{P} = \frac{\mp 2\hat{\vec{Q}}(\hat{\vec{Q}} \cdot \hat{\vec{m}}) - \vec{P}_0[1 + (\hat{\vec{Q}} \cdot \hat{\vec{m}})^2] + 2\vec{M}_x(\vec{M}_x \cdot \vec{P}_0) + 2\vec{M}_y(\vec{M}_y \cdot \vec{P}_0)}{1 + (\hat{\vec{Q}} \cdot \hat{\vec{m}})^2 \pm 2(\vec{P}_0 \cdot \hat{\vec{Q}})(\hat{\vec{Q}} \cdot \hat{\vec{m}})} \quad (16)$$

with $\vec{M}_x = \hat{\vec{x}} - (\hat{\vec{x}} \cdot \hat{\vec{Q}})\hat{\vec{Q}}$ and a similar definition can be written for \vec{M}_y . $\hat{\vec{x}}$ and $\hat{\vec{y}}$ are chosen to be perpendicular to $\hat{\vec{m}}$. Equation 16 tells us that the final polarization of the neutron depends on the direction of its initial polarization and on the relative orientation of the magnetization

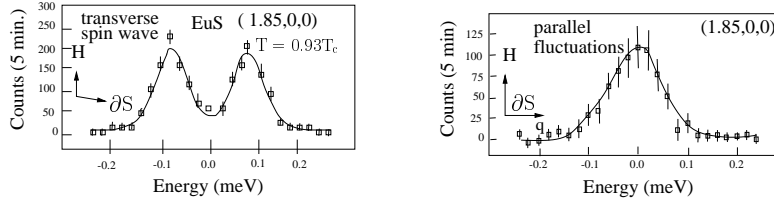


Figure 3: *Left*: Spin waves in EuS, spin-flip channel. *Right*: Longitudinal fluctuations in EuS, non spin-flip channel (Taken from Ref. [12]).

with the scattering vector \vec{Q} . In particular, if an external magnetic field is applied perpendicular to the scattering plane and is strong enough to align the magnetic domains, both the magnetization vector and the initial polarization are aligned along the field. In that case, the spin of the neutrons will be reversed when neutrons are scattered by the spin waves. On the contrary, the longitudinal fluctuations will not influence the spin of the neutrons. Therefore, for that particular scattering geometry, the spin waves in EuS will occur in the '*spin-flip channel*', while the longitudinal fluctuations will be '*non spin-flip*', as shown in Fig. 3.

2.2 Ferrimagnets and antiferromagnets

So far we have considered magnetic systems which contain one ion in the magnetic cell. For compounds with many magnetic sublattices, like ferrimagnets and antiferromagnets, the spectrum of the magnetic excitations has more than one dispersion branch $\omega(\vec{k})$, like phonons in crystals. As an example, we will consider here the spin-wave spectrum of CuFe_2O_4 . Cubic CuFe_2O_4 crystallizes in the spinel structure (space group $Fd\bar{3}m$) with eight sites of tetrahedral symmetry (A-sites) and sixteen sites of octahedral symmetry in the unit cell. The magnetic structure of CuFe_2O_4 is ferrimagnetic below $T_c \sim 750\text{K}$. If annealed in air and slowly cooled from 740°C , it undergoes a tetragonal distortion ($c/a=1.09$) below $T = 650\text{K}$.

The structural phase transition is driven by the cooperative Jahn-Teller effect that tends to distort the octahedron to lift the degeneracy of the doubly degenerate electronic ground-state of the Cu^{2+} ions. The

valence state of copper is +2, so that every Cu carries an effective spin $S=1/2$. Fe is in the +3 oxidation state in CuFe_2O_4 and, accordingly, has a spin $S=5/2$. To obtain the spectrum of magnetic excitations, spin-wave theory can be used. The Heisenberg operator must now take into account that CuFe_2O_4 has two magnetic sublattices with different spins, $S_A \sim 1/2$ and $S_B \sim 5/2$,

$$H = \sum_{i,j} J_{i,j}^A \vec{S}_i^A \cdot \vec{S}_j^A + \sum_{i,j} J_{i,j}^B \vec{S}_i^B \cdot \vec{S}_j^B + \sum_{i,j} J_{i,j}^{AB} \vec{S}_i^A \cdot \vec{S}_j^B + \sum_{i,j} J_{i,j}^{BA} \vec{S}_i^B \cdot \vec{S}_j^A \quad (17)$$

The equations of motion for the spins in the A- and B-sublattices are similar to the ones which were derived for the simple ferromagnet. However, the calculations which lead to the spin-wave dispersion are rather lengthy and will not be reproduced here. A complete derivation of the spin-wave spectrum for a two sublattices ferrimagnet can be found *e.g.* in the book of Turov [13]. The result yields

$$\begin{aligned} \hbar\omega_{1,2}(\vec{k}) = & \pm[(S_B - S_A)J^{A,B}(0) - S_A(J^A(0) - J^A(\vec{k})) + S_B(J^B(0) \\ & - J^B(\vec{k}))] + \frac{1}{2}\{[2(S_B + S_A)J^{A,B}(0) - 2S_A(J^A(0) - J^A(\vec{k})) \\ & - 2S_B(J^B(0) - J^B(\vec{k}))]^2 - S_AS_B(4J^{A,B}(\vec{k}))^2\}^{1/2}. \end{aligned} \quad (18)$$

Two branches of spin waves appear in the spectrum of excitations in a ferrimagnet. At the magnetic zone center, one branch exhibits a gap, while the other one goes to zero like k^2 . Setting $S^A = S^B = S$ and $J^A = J^B = J$ in Eq. 18, the dispersion relation for a simple collinear antiferromagnet with next-nearest neighbor exchange interactions is obtained,

$$\hbar\omega_{1,2}(\vec{k}) = 2S\sqrt{(J^{A,B}(0) - J(0) - J(\vec{k}))^2 - [J^{A,B}(\vec{k})]^2} \quad (19)$$

From Eq. 19 it is seen that the spectrum of the magnetic excitations of an isotropic antiferromagnet is doubly degenerate and goes to zero at the magnetic zone center. La_2CuO_4 is a typical example of an Heisenberg antiferromagnet. The dispersion of the magnetic excitations in this compound is in agreement with Eq. 19, as shown in Fig. 4.

2.3 The role of the anisotropy

The spin-spin interactions between electrons like the direct exchange in ferromagnets and the 'super'-exchange interactions in antiferromagnets are described by an effective bilinear Hamilton operator where

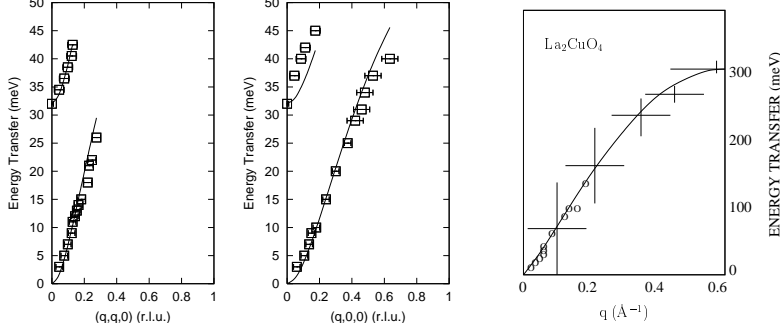


Figure 4: *Left, Center*: Dispersion of the spin waves in CuFe_2O_4 at $T=300\text{K}$. The line is the result of calculations using Eq. 18 with $J^{A,B} = -1.2\text{meV}$ and $J^A = J^B \sim 0\text{meV}$. (Ref. [10]). *Right*: Dispersion of the spin waves in La_2CuO_4 (Taken from Ref. [11]).

the exchange integrals are only functions of the distance between the ions, $J(\vec{r}_i - \vec{r}_j) = J(|\vec{r}_i - \vec{r}_j|)$. However, higher-order terms in the spin Hamiltonian are possible [14] and, in general, the spin-spin Hamiltonian can be expanded in a power series of the spin operators

$$H = \sum_{i,j} J_{i,j}^{\alpha,\beta} S_i^\alpha S_j^\beta + \sum_{i,j,k,l} J_{i,j,k,l}^{\alpha,\beta,\delta,\gamma} S_i^\alpha S_j^\beta S_k^\delta S_l^\gamma + \dots \quad (\alpha, \beta, \delta, \gamma = x, y, z) \quad (20)$$

Which terms are of significance for a particular physical problem depends on the lattice symmetry and most often higher order powers in Eq. 20 give only a small contribution to the magnetic energy. We show in Fig. 5 the result of measurements of the spin-wave excitations in Li_2CuO_2 which is a three-dimensional collinear antiferromagnet below $T_N = 9.2\text{K}$. The model Hamiltonian used to describe the dispersion of the spin waves in Li_2CuO_2 consists of the Heisenberg operator including uniaxial anisotropy along the spin direction

$$H = \sum_{i,j} J_{i,j} \vec{S}_i \cdot \vec{S}_j + \sum_{i,j} J_{i,j}^\perp S_i^z S_j^z. \quad (21)$$

The corresponding dispersion relation of the spin waves is given by $\hbar\omega(\vec{k}) = S\sqrt{(I(\vec{k}) + J(0) - I(0) + D)^2 - J^2(\vec{k})}$ with $D = J^\perp(0) -$

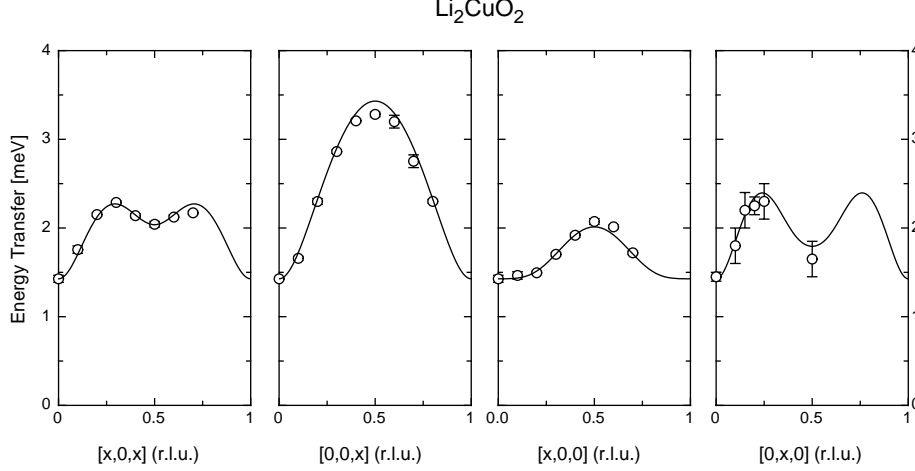


Figure 5: Dispersion of the spin waves in Li_2CuO_2 at $T=1.5\text{K}$ (After Ref. [15]).

$I^\perp(0)$ where $J(\vec{k})$ and $I(\vec{k})$ are the inter- and intra-sublattice exchange integrals, respectively [15]. A single spin-wave branch characterized by a large energy-gap is obtained. The gap in the spectrum of the magnetic excitations of Li_2CuO_2 is the result of the presence of the strong anisotropy which aligns the magnetic moments along the easy-axis of magnetization. It has been shown that magnetic anisotropy in this case results from second order spin-orbit coupling which induces anisotropic super-exchange interactions in 90° Cu-O-Cu bonds as it is realized in Li_2CuO_2 and in cuprates with edge-sharing CuO_2 chains [16].

Other sources of magnetic anisotropies originate from the electric field produced by the atoms surrounding a magnetic ion. The form of the crystal field Hamiltonian depends on the symmetry of the lattice. For tetragonal symmetry, the single-ion anisotropy has the form $H_A = D \sum_j [(S_j^z)^2 - \frac{1}{3}S(S+1)]$. Moriya has shown that the spin-orbit coupling introduces an effective interaction between the spins of the form $H_{DM} = \vec{D} \cdot \sum_{i,j} (\vec{S}_i \times \vec{S}_j)$ in compounds without inversion center. In some special cases, the anisotropy might be so large, that the magnetic properties of a compound are well described by either an Ising-like ($H = \sum_{i,j} S_i^z S_j^z$) or an XY-like ($H = \sum_{i,j} (S_i^x S_j^x + S_i^y S_j^y)$) model. Table 1 gives a summary of typical substances and of the

corresponding models used to account for their magnetic properties.

Table 1: Some compounds that show characteristic Heisenberg, Ising or XY-behavior (after Reference [17]). D is the dimension of the lattice (D=3: three-dimensional lattice; D=2: layered structures; D=1: spin chains)

D	Heisenberg	Ising	XY
3	EuO, EuS, RbMnF ₃ , KMnF ₃	Tb(OH) ₃ , DyPO ₄ , FeF ₂	Co(C ₅ H ₅ NO ₆)(ClO ₄) ₂ Fe[Se ₂ CN(C ₂ H ₅) ₂] ₂ Cl
2	K ₂ CuF ₄ , BaMnF ₄ K ₂ NiF ₄	FeCl ₂ , CoCs ₃ Br ₅ , RbCoF ₄	CoBr ₂ · 6H ₂ O CoCl ₂
1	(C ₆ H ₁₁ NH ₃)CuBr ₃ RbNiCl ₃ , CsNiCl ₃	CoCl ₂ · 2H ₂ O CsCoCl ₃ , RbFeCl ₅ · 2H ₂ O	(CH ₃) ₄ NNiBr ₃ Cs ₂ CoCl ₄ , PrCl ₃

3 Excitations in itinerant electron magnetism

The Heisenberg model is based on the assumption that the magnetic moments are localized around the ions and that the value of the spin is a multiple half-integer of a Bohr magneton μ_B . However, metallic compounds like Fe, Co or Ni have magnetic moments of $\sim 2.12\mu_B$, $\sim 1.57\mu_B$ and $\sim 0.6\mu_B$, respectively. To account for this effect, it must be recognized that in a metal electrons are 'delocalised' and arrange themselves in the lattice in electronic bands. This corresponds to the case where in the Hubbard model the kinetic energy t is much larger than the inter-site Coulomb energy U . Although the (t, U) phase-diagram in three-dimensions is not exactly known, it can be shown that in the limit where $t \gg U$ and within the mean-field approximation, the Hubbard model reproduces the Stoner theory of ferromagnetism [2].

3.1 Stoner Theory

The Stoner theory proceeds in a similar way as the Pauli theory of paramagnetism. However, it includes the Coulomb repulsion. The

energy of an electron in the presence of an external magnetic field H and of exchange interactions U_{ex} is given by $\epsilon_k = \frac{\hbar^2 k^2}{2m} \mp \frac{1}{2}(U_{ex}M + gH\mu_B)$, where $M = n_\uparrow - n_\downarrow$ is the magnetization and \mp refers to the band with spin-up and -down, respectively. The energy bands are split by an energy $U_{ex}M + H\mu_B$, which in the absence of a magnetic field is proportional to the magnetization. This is called the exchange splitting. As a response to the action of both the external field and of the exchange interaction, the system develops a spin polarization. The static susceptibility $\chi = \frac{\partial M}{\partial H}$ is accordingly given by [2]:

$$\chi = \frac{(g\mu_B)^2 \rho(\epsilon_F)}{2} \cdot \frac{1}{1 - U_{ex}\rho(\epsilon_F)} = \frac{\chi_{Pauli}}{1 - U_{ex}\rho(\epsilon_F)}. \quad (22)$$

$\rho(\epsilon_F)$ is the density of the electrons at the Fermi level. $S_{Stoner} = 1/(1 - U_{ex}\rho(\epsilon_F))$ is called the '*Stoner enhancement factor*'. The susceptibility of an interacting electron gas is enhanced by the factor S_{Stoner} compared to the Pauli susceptibility χ_{Pauli} of the free electron system. When $U\rho(\epsilon_F) \approx 1$ the susceptibility diverges and a phase transition to an ordered ferromagnetic state occurs. A calculation based on electronic band calculations taking into account exchange correlation energies is shown in Table 2. The results show that ferromagnetism in Fe, Co and Ni is explained within the frame of the Stoner theory. A great success of the Stoner theory is that it relates both the value of the magnetic moment at $T = 0K$ and the Curie temperature T_c to the enhancement factor S_{Stoner} ,

$$M(0) = \sqrt{-S_{Stoner}\rho^3(\epsilon_F)/a} \quad (23)$$

$$T_c = \frac{\sqrt{3}}{\pi k_B} \sqrt{-S_{Stoner}\rho(\epsilon_F)/a}, \quad (24)$$

with a the lattice constant. Accordingly, materials with a large Stoner enhancement factor are expected to order ferromagnetically at high temperatures and to have a large magnetization at saturation, in agreement with experimental values tabulated in Table 2 for some typical metallic compounds.

3.2 Dynamical susceptibility

Materials for which $U_{ex}\rho(\epsilon_F)$ is close to the critical value of 1 (like Pd) are called '*nearly ferromagnets*'. The imaginary part of the dynamical

Table 2: Stoner enhancement factor from electronic band-calculations (after Refs. [17],[18])

	$U_{ex}\rho(\epsilon_F)$	S_{Stoner}	T_c (K)
Al	0.25	1.71	-
α -Fe	1.43	-2.34	1044
Co	1.70	-1.43	1390
Ni	2.04	-0.97	624
Cu	0.11	1.12	-
Pd	0.78	4.44	-

susceptibility is enhanced by the exchange interaction, so that fluctuations in such paramagnetic metals are directly accessible by inelastic neutron scattering as,

$$\Im\chi(\vec{k}, \omega) = \omega\chi(\vec{k}) \frac{\Gamma(\vec{k})}{\omega^2 + \Gamma^2(\vec{k})}, \quad (25)$$

where $\chi^{-1}(\vec{k}) = \chi^{-1} + ck^2$ is the inverse static susceptibility and $\Gamma(\vec{k}) = \gamma\chi(\vec{k})$ is a characteristic relaxation frequency. The microscopic constants c and γ characterize the static and dynamic parts of the dynamical susceptibility and can be calculated from the electronic-band structure [19]. Ni₃Ga is a classical example of a paramagnetic metal with strongly correlated 3d transition electrons and exchange enhanced susceptibility. The imaginary part of the dynamical susceptibility as measured with inelastic neutron scattering is consistent with Eq. 25, which is characterized by a strong rise of the scattering intensity at low k and ω [20], as shown in Fig. 6.

ZnZr₂ is characterized by an exchange enhancement factor that is just above the critical value, namely $U_{ex}\rho(\epsilon_F) = 1.015$. ZrZn₂ orders ferromagnetically at $T_c \sim 25$ K and the magnetic moment at saturation is $\mu = 0.12\mu_B$. There exists a large class of such materials which order at low temperature with very small ordered magnetic moments called '*Weak Ferromagnets*'. For these materials, and in the ferromagnetic phase, the spectrum of magnetic excitations consists of well-defined spin waves at small values of \vec{k} that merge into a continuum of excitations ('*Stoner Continuum*') at large values of momentum

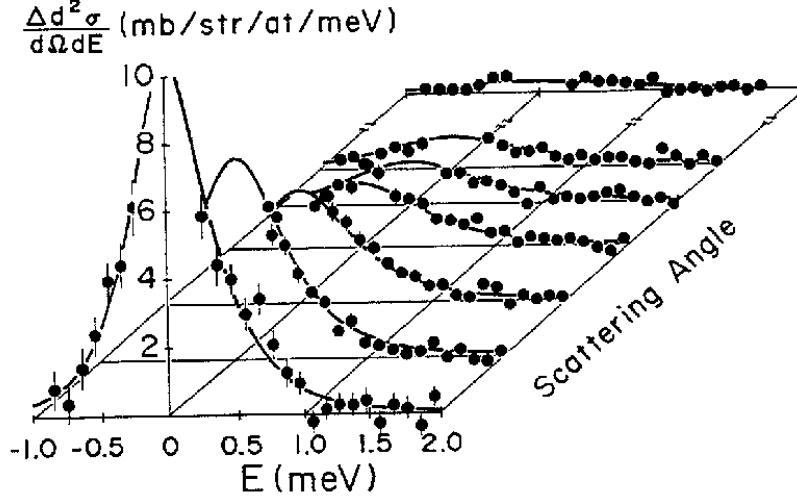


Figure 6: Energy dependence of the scattering intensity in the paramagnetic metal Ni_3Ga (taken from Ref. [20]).

transfers. The dispersion of the spin-waves is quadratic $\hbar\omega(\vec{k}) = Dk^2$. D is the stiffness constant and is proportional to the magnetization, namely $D = 2\mu_B cM$ [21]. As an example, Fig. 7, shows the dispersion of the magnetic excitations in Ni_3Al that is also a typical weak ferromagnet with $T_c = 72K$ and $\mu = 0.075\mu_B$.

The neutron cross-sections for magnetic excitations in the Stoner continuum are quite involved and can be found in Ref. [3]. Fig. 8 shows the dispersion and the intensity of a ferromagnetic electron gas. It is seen, that the neutron intensity decreases upon entering the Stoner continuum and the line shape of the magnetic excitations significantly increases. This is in agreement with neutron scattering studies in Fe, Ni [23] and MnSi [24].

3.3 Generalized Susceptibility

The Stoner theory is based on the free electron model with Coulomb interactions. For real shapes of the Fermi surfaces in metals, the static

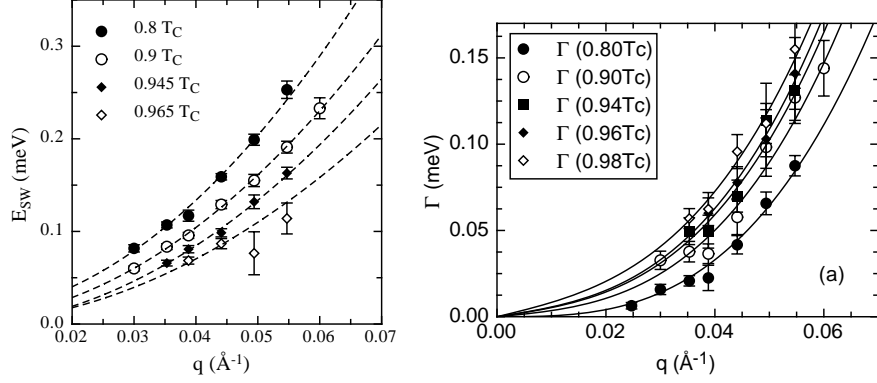


Figure 7: *Left*: Dispersion of the magnetic excitations in Ni_3Al as a function of temperature. *Right*: Dependence of the line-width of the spin-wave excitations in Ni_3Al as a function of momentum transfer. See Ref. [22] for details.

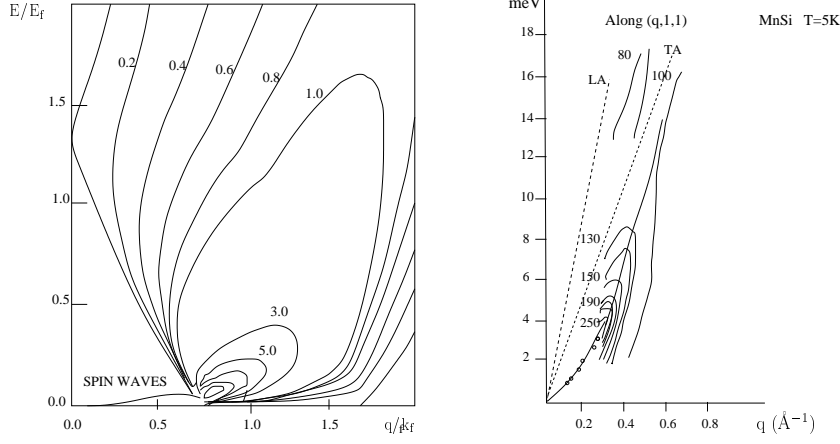


Figure 8: *Left*: Dispersion of the magnetic excitations in a ferromagnetic gas. The contour lines refer to the imaginary part of the dynamical susceptibility. *Right*: Dispersion of the magnetic excitations in MnSi at $T=5\text{K}$ and $H=10\text{kOe}$. Reproduced from Ref. [24]. Note the quadratic dispersion of the spin waves and the Stoner continuum above $\hbar\omega \sim 3\text{meV}$.

susceptibility of Eq. 22 is \vec{k} -dependent

$$\chi(\vec{k}) = (g\mu_B)^2 \frac{\chi^0(\vec{k})}{1 - U_{ex}\chi^0(\vec{k})}, \quad (26)$$

where $\chi^0(\vec{k})$ is not the Pauli-susceptibility anymore but depends on the details of the electronic band structure [25]. Similarly to the case of ferromagnetism, the system can undergo a phase transition if U_{ex} is large enough. If the Lindhard-function for free electrons in three-dimensions is chosen for $\chi^0(\vec{k})$, the generalized static susceptibility diverges for $\vec{k} \rightarrow 0$ that corresponds to the on-set of ferromagnetism. In the general case, the susceptibility can diverge at any value of \vec{k} , which leads to the formation of spin-density waves. A well-known example is chromium which undergoes a phase-transition to an incommensurate phase at $T_N = 311\text{K}$. The enhancement factor $1 - U_{ex}\chi^0(\vec{k}) \approx 1.025$ is only slightly above the critical value. The incommensurate spin-density wave structure of Cr associated with wave vector $\vec{k}_0 = (0, 0, \sim 0.96)$ can be ascribed to nesting of the Fermi surface [26]. The theory of the magnetic excitations in weakly anti-ferromagnetic and helimagnetic metals was developed by Moriya and is similar to the ferromagnetic case. We refer to the book of Moriya for details [21].

4 Conclusions

Inelastic neutron scattering is a powerful means for the investigation of spin waves and spin fluctuations in magnetic materials. Starting with the Heisenberg model we have shown that a measurement of the dispersion relation of the spin waves allows a direct determination of the exchange constants between the magnetic moments. Close to the critical temperature the spin deviations from the magnetisation direction \vec{M} become large leading to a damping of the spin waves and thus to the appearance of longitudinal fluctuations along \vec{M} . These modes can be separated by means of polarisation analysis.

In general, crystal field effects, dipolar and spin-orbit interactions etc. lead to higher order terms in the Hamiltonian which can lead to the appearance of an energy gap and/or lift the degeneracy of the spin-wave modes. Systems with more than one magnetic moment per unit cell show several dispersion branches.

The picture of localised moments breaks down as soon as the carriers of the magnetic moments interact or become part of the sea of conduction electrons. Here, a description of the spin fluctuations in terms of itinerant models is more appropriate. Neutron scattering shows directly that spin waves exist at small \vec{k} merging into a sea of single-particle (Stoner) excitations at larger \vec{k} . In nearly ferromagnetic materials the low energy fluctuations are dramatically enhanced.

In summary, inelastic neutron scattering is at present the only method to measure spin fluctuations over a large range of \vec{k} and ω in localised and itinerant systems. It has provided invaluable input for a better understanding of the interactions in weakly and strongly correlated materials that are of current interest in the field of high- T_c superconductions, colossal magneto-resistance materials and heavy-fermion system. Due to limitations in space we refer the reader to the specialized literature on these subjects.

References

- [1] J. Hubbard, Proc. Roy. Soc. London **A 276**, 238 (1963).
- [2] see e.g. P. Fazekas in *Lecture Notes on Electron Correlation and Magnetism*, Series in Modern Condensed Matter Physics. Vol. 5 (1999).
- [3] Stephen W. Lovesey in *Theory of Neutron Scattering from Condensed Matter*, Clarendon Press Oxford (1984).
- [4] H.G. Bohn, W. Zinn, B. Dorner, and A. Kollmar, Phys. Rev. B **22**, 5447 (1980).
- [5] P.Böni, M. Hennion, and J.L. Martínez, Phys. Rev. B **52**, 10142 (1995).
- [6] T. Holstein and H. Primakoff, Phys. Rev. **58**, 1098 (1940).
- [7] F. Schwabl, Z. Phys. **246**, 13 (1971).
- [8] M. Blume, Phys. Rev. **130**, 1670 (1963).
- [9] R.M. Moon, T. Riste, and W.C. Koehler, Phys. Rev. **181**, 920 (1969); Yu A. Izyumov and S.V. Maleev, Soviet Phys. JETP **14**, 1168 (1962).
- [10] B. Roessli, G. Petakovskii, A. Krimmel, L. Capogna and T. Chatterji, unpublished.

- [11] S.M. Hayden *et al.*, Phys. Rev. Lett. **67**, 3622 (1991).
- [12] P. Böni, B. Roessli, D. Görlitz, J. Kötzler, and J.L. Martínez, Proc. IAEA TCM, Neutron Beam Research, ITN Lisbon, 68 (1997).
- [13] E.A. Turov, *Physical Properties Of Magnetically Ordered Crystals*, Academic Press (New York and London) 1965.
- [14] S.V. Tyablikov, *Methods in the Quantum Theory of Magnetism*, Plenum Press, New-York (1967).
- [15] M. Boehm, S. Coad, B. Roessli, A. Zheludev, M. Zolliker, P. Böni, D. McK. Paul, H. Eisaki, N. Motoyama, and S. Uchida, Euro. Phys. Lett. **43**, 77 (1998).
- [16] V. Yu. Yushankhai and R. Hayn, Euro. Phys. Lett. **47**, 116 (1999); N. Tanaka, M. Suzuki, and K. Motizuki, J. Phys. Soc. Japan **68**, 1684 (1999).
- [17] E. Jäger and R. Perthel, *Magnetische Eigenschaften von Festkörpern*, Akademie Verlag, 1996.
- [18] Walter A. Harrison, *Electronic Structure And The Properties Of Solids*, Dover Publications, Inc., New-York 1989.
- [19] G.G. Lonzarich and L. Taillefer, J. Phys. C: Solid State Phys. **18**, 4339 (1985).
- [20] N. Bernhoeft, S.M. Hayden, G.G. Lonzarich, D. McK Paul, and E.J. Lindley, Phys. Rev. Lett., **62**, 657 (1989).
- [21] T. Moriya, '*Spin Fluctuations in Itinerant Electron Magnetism*', Springer Series in Solid-State Sciences **56**, Springer-Verlag 1985.
- [22] F. Semadeni, B. Roessli, P. Böni, P. Vorderwisch, and T. Chatterji, Phys. Rev. B **62**, 1083 (2000).
- [23] H.A. Mook, R.M. Nicklow, E.D. Thompson, and M.K. Wilkinson, J. Appl. Phys. **40**, 1450 (1969); H.A. Mook and D.McK. Paul, Phys. Rev. Lett. **54**, 227 (1985).
- [24] Y. Ishikawa, Y. Uemura, F. Majkrzak, G. Shirane, and Y. Noda, Phys. Rev. B **31**, 5884 (1985).
- [25] A.W. Overhauser, Phys. Rev. Lett. **4**, 462 (1960); I.E. Dzyaloshinskii, Sov. Phys. JETP, 223 (1965).
- [26] W.M. Lomer, Proc. Phys. Soc. A **80**, 489 (1962); J. Rath and J. Callaway, Phys. Rev. B **8**, 5398 (1973).